Nuclear Medicine and Molecular Imaging (2020) 54:86–97
https://doi.org/10.1007/s13139-020-00640-z

REVIEW

ISSN (print) 1869-3482
ISSN (online) 1869-3474

Preclinical Voxel-Based Dosimetry in Theranostics: a Review

Arun Gupta[1] · Min Sun Lee[2] · Joong Hyun Kim[3] · Dong Soo Lee[4] · Jae Sung Lee[4,5,6]

Received: 22 January 2020 / Revised: 27 March 2020 / Accepted: 31 March 2020 / Published online: 19 April 2020

Abstract

Due to the increasing use of preclinical targeted radionuclide therapy (TRT) studies for the development of novel theranostic agents, several studies have been performed to accurately estimate absorbed doses to mice at the voxel level using reference mouse phantoms and Monte Carlo (MC) simulations. Accurate dosimetry is important in preclinical theranostics to interpret radiobiological dose-response relationships and to translate results for clinical use. Direct MC (DMC) simulation is believed to produce more realistic voxel-level dose distribution with high precision because tissue heterogeneities and nonuniform source distributions in patients or animals are considered. Although MC simulation is considered to be an accurate method for voxel-based absorbed dose calculations, it is time-consuming, computationally demanding, and often impractical in daily practice. In this review, we focus on the current status of voxel-based dosimetry methods applied in preclinical theranostics and discuss the need for accurate and fast voxel-based dosimetry methods for pretherapy absorbed dose calculations to optimize the dose computation time in preclinical TRT.

Keywords Preclinical · Voxel-based dosimetry · Theranostic · ^{177}Lu · Monte Carlo

Introduction

Small animals, especially mice, have been increasingly used in preclinical research to develop novel theranostic agents and treatment modalities for human diseases, including cancer [1, 2]. Cancer treatment methods are typically based on the use of ionizing radiation, e.g., external beam radiotherapy (EBRT), brachytherapy, and radionuclide therapy. Recently, targeted radionuclide therapy (TRT), especially peptide receptor radionuclide therapy (PRRT), has gained increasing importance in the treatment of various cancers, including lymphoma, glioblastoma, neuroendocrine tumors, and prostate cancer with distant metastases [3–7]. TRT can simultaneously target primary tumor sites and distant metastatic disease that remains undetectable by diagnostic imaging [8]. Selective uptake and prolonged retention of the radiopharmaceutical within the tumor are required for successful PRRT [9]. Several new radiolabeled peptides are being developed to target specific receptors that are overexpressed in various cancers, such as glioma, ovarian cancer, neuroendocrine tumor, and cervical cancer [10, 11]. Such peptides are useful because normal human organs and tissues exhibit very limited expression of these receptors.

All cancer therapies that use ionizing radiation, including TRT, share a common goal: to deliver the highest possible absorbed dose to the tumor while sparing healthy tissues to achieve the highest therapeutic efficacy. To fulfill this objective, the careful selection of radionuclides combined with specific vectors is required to target the cancer cells. Many peptides conjugated with theranostic radionuclides, such as ^{177}Lu and ^{188}Re, have been considered valuable tools for novel and effective anti-cancer therapies [12]. Despite the excellent tumor targeting ability of these radiolabeled peptides, there is

✉ Jae Sung Lee
jaes@snu.ac.kr

Arun Gupta
arunaiims1984@gmail.com

1 Department of Radiology & Imaging, B.P. Koirala Institute of Health Sciences, Dharan, Nepal

2 Department of Radiology, School of Medicine, Stanford University, Stanford, CA, USA

3 Center for Ionizing Radiation, Korea Research Institute of Standards and Science, Daejeon, South Korea

4 Department of Nuclear Medicine, College of Medicine, Seoul National University, 103 Daehak-ro, Jongno-gu, Seoul 03080, South Korea

5 Interdisciplinary Program in Radiation Applied Life Science, Seoul National University, Seoul, South Korea

6 Department of Biomedical Sciences, College of Medicine, Seoul National University, Seoul, South Korea

always a risk of renal and bone marrow toxicity due to the particulate radiation emitted from the theranostic radionuclides [13–15]. Therefore, internal dosimetry for absorbed dose calculation is essential to obtain absorbed dose-response relationships during clinical and preclinical TRT for the evaluation of therapeutic outcomes and toxicities [16–18]. However, accurately assessing the absorbed dose in tumors and normal organs or tissues during TRT treatment planning remains challenging [19–21].

Absorbed doses in small animals can be calculated using a Medical Internal Radiation Dose (MIRD) scheme if animal-specific *S* values (mean absorbed dose in a target organ per radioactivity decay in a source organ) are determined [22–24]. However, an organ-level MIRD method does not consider patient- or animal-specific anatomies and activity distributions because it assumes that there are homogeneous activity distributions in organs and a generalized geometry [25, 26]. Therefore, the inclusion of nonuniform activity distributions and tissue heterogeneity has been considered important for more accurate absorbed dose calculations at the voxel level [26–30]. This article reviews the current status of preclinical voxel-based dosimetry methods applied in theranostics and discusses the need for accurate and fast dosimetry methods to calculate pretherapy absorbed dose at the voxel level to optimize the dose computation time in preclinical TRT.

Radionuclides for Preclinical TRT

The selection of radionuclides is crucial in TRT treatment planning and should be performed individually, based on the characteristics of the tumor, adjacent tissues, and affinity for the targeting compound. The radionuclides that emit particulate radiation (α, β, and Auger) are of primary interest for TRT to cause non-reparable DNA damage by radiation-induced ionization [31, 32]. Because peptides are internalized, the physical and chemical characteristics of the radionuclides used in TRT should be fully explored [19]. Physical properties of radionuclides that are important for clinical and preclinical applications are mode of production, half-life, type of emission, particle energy, the maximum range of particles emitted, and linear energy transfer (LET).

Although many radioisotopes can be used as radiation sources, only a few have been developed and applied in preclinical and in vivo studies; these include ^{111}In, ^{68}Ga, ^{64}Cu, ^{90}Y, ^{188}Re, and ^{177}Lu. Due to their inherent theranostic natures, ^{177}Lu and ^{188}Re are used for both diagnostic and therapeutic purposes [33]. The shorter tissue penetration range of ^{177}Lu may reasonably exert a more favorable effect on small tumors compared with ^{90}Y and ^{188}Re [19]. Radionuclides that emit gamma emission are desirable in theranostics because monitoring of in vivo radiopharmaceutical distribution as well as the assessment of pre- and post-therapy dosimetry is possible. Radionuclides used in diagnostics emit a large fraction of distributed radiation energy, whereas radionuclides for therapy are designed to deposit the energy from radioactive decay locally [34]. A list of common therapeutic radionuclides with their physical properties and applications is presented in Table 1.

Imaging Modalities for Preclinical TRT and Dosimetry

During the preclinical development of radiopharmaceuticals, numerous small animals are injected with radioactive agents and sacrificed at different time points to obtain biodistribution data of the injected radiopharmaceutical for the assessment of toxicity and efficacy [16]. Recently, due to the advancement in high-resolution radionuclide imaging, a variety of small-animal single-photon emission computed tomography (SPECT) and positron emission tomography (PET) protocols were developed for preclinical imaging studies of radiolabeled peptides and antibodies to investigate disease development and therapy response [35–38]. PET imaging for small animals has been considered more accurate for quantitative studies due to its higher sensitivity and good spatial resolution [39, 40]. SPECT provides three-dimensional (3D) spatial information; however, physical quantities such as photon attenuation, scattering, and partial volume errors influence the absolute quantification of SPECT images [41].

Several researchers have proposed different techniques to solve these issues. Consequently, preclinical SPECT/CT cameras with multi-pinhole collimators have been developed to increase system sensitivity while maintaining good spatial resolution [42–45]. Finucane et al. [46] conducted phantom imaging using ^{111}In and ^{99m}Tc sources and obtained quantitatively accurate information from a multi-pinhole SPECT/CT camera to assess radiotracer biodistribution in mouse models; these assays can replace conventional dissection studies. Gupta et al. [47] performed several phantom studies using ^{177}Lu and ^{99m}Tc to evaluate the system performance of a multi-pinhole SPECT/CT and found that the parameters evaluated are suitable for obtaining quantitatively accurate SPECT images of mice for personalized dosimetry in preclinical ^{177}Lu PRRT. The CT-derived anatomic information obtained from integrated SPECT/CT improves SPECT quantification and organ delineation in TRT, which is an essential step in 3D voxel-based dosimetry [26, 48].

Organ-Level Internal Dosimetry

Internal dosimetry is the method of absorbed dose calculation in a volume of interest (i.e., whole organ, tumor, or voxel) from internally distributed radionuclides in radionuclide

Table 1 Common therapeutic radionuclides with their physical properties and applications (maximum energy and particle range in tissues are reported for beta emission)

Radionuclide	Half life (physical)	Useful emissions	Energy	Particle range in tissue (R_{max})	Application
^{188}Re	16.9 h	β^-	$E_{max,\ \beta^-}$: 2.12 MeV	11 mm	Theranostics
		γ	E_γ: 155 (10%) keV		
^{177}Lu	6.73 days	β^-	$E_{max,\ \beta^-}$: 0.498 MeV	2 mm	Theranostics
		γ	E_γ: 208 (11%), 113 (6%) keV		
^{166}Ho	28.8 h	β^-	$E_{max,\ \beta^-}$: 1.85 MeV	8.7 mm	Theranostics
		γ	E_γ: 81 (7%) keV		
^{153}Sm	46.5 h	β^-	$E_{max,\ \beta^-}$: 0.805 MeV	0.33 mm	Theranostics
		γ	E_γ: 103 (28%), 70 (5%) keV		
^{131}I	8.02 days	β^-	$E_{max,\ \beta^-}$: 0.606 MeV	0.42 mm	Theranostics
		γ	E_γ: 364 (81%), 637 (7%) keV		
^{111}In	67.4 h	γ	E_γ: 173 (83%), 247 (94%) keV	10 μm	
		e^- Auger	E: 0.5–25 keV	550 μm	
		e^- IC	E: 144–245 keV		Theranostics
^{90}Y	64.1 h	β^-	$E_{max,\ \beta^-}$: 2.28 MeV	11.3 mm	Therapy only
^{89}Sr	50.5 days	β^-	$E_{max,\ \beta^-}$: 0.583 MeV	0.7 mm	Therapy only
^{64}Cu	12.8 h	β^-	$E_{max,\ \beta^-}$: 0.570 MeV	2.5 mm	Theranostics
		β^+	$E_{max,\ \beta^+}$: 0.653 MeV	0.7 mm	

imaging and therapy. The absorbed dose of each organ depends on the physical properties of the radionuclide, the injected activity, and the kinetics of uptake and clearance of radioactivity within the tumor and normal tissue or cells [49].

The method for calculating the absorbed dose of radiation from internal sources was formulated by the MIRD committee of the Society of Nuclear Medicine in the 1960s [50]. MIRD is a dosimetry method that uses S values (mean absorbed dose in a target organ per radioactivity decay in a source organ), also known as dose factors released by the Radiation Dose Assessment Resource (RADAR) group, especially for human organ sizes and relationships [30, 50, 51]. According to the MIRD schema [30], the average absorbed dose $D(r_T, T_D)$ is given by

$$D(r_T, T_D) = \sum_{r_s} \int_0^{T_D} \widetilde{A}\ (r_s, t)\ S(r_T \leftarrow r_s) dt, \quad (1)$$

where r_T is the target organ, and $\widetilde{A}\ (r_s, t)$ is the time-integrated activity in source organ r_s over the dose integration period, T_D.

The absorbed dose in small animals can be calculated using the MIRD schema if murine-specific S values are supplied [16, 22–24, 52]. However, the application of the MIRD method for the calculations of absorbed dose in mice is not direct because the size and relationship of mouse organs are significantly different than those of humans [27, 28, 53]. In addition, the anatomical difference between humans and mice becomes more important when the dosimetry is performed for beta-emitting radionuclides. The cross-beta absorbed dose should be considered when using MIRD formalism for mouse dosimetry because the size of organs in mice and the range of beta particles are the same order of magnitude. In addition, organs are very close to each other in mice [54, 55].

Based on the MIRD formalism and RADAR method of dose calculation, several dosimetry applications were developed. MIRDOSE [56] and Organ Level Internal Dose Assessment/Exponential Modeling (OLINDA/EXM) [57] are the most widely used fixed geometry dosimetry software packages. Organ-level dosimetry applications based on standard phantoms are inadequate for absorbed dose calculations in TRT because they do not incorporate patient-specific or tumor dosimetry. However, OLINDA/EXM is capable of modeling simple tumors in the form of unit density spheres of various sizes based on the absorbed fractions by assuming uniform activity distributions [58]. Because it is not always possible to model the size, shape, and location of every unique tumor with the reference phantoms used in OLINDA/EXM, this approach does not provide information about the 3D dose distribution in tumors [57–59].

Voxel-Level Dosimetry Using a MIRD Schema

Absorbed dose calculations can also be performed at the voxel level. Several researchers have addressed the limitations associated with organ-level dosimetry, and various steps have been taken to extend the MIRD schema to absorbed dose calculations at the voxel level by using voxel S values [29, 30]. MIRD pamphlet no. 17 [29] summarizes the methods of voxel-based dosimetry using voxel S values in the MIRD formalism that require the assessment of the 3D distribution

of the radiopharmaceutical within the body. According to Bolch et al. [29], mean absorbed dose D to a given target voxel k from N surrounding source voxels h (including the target voxel itself, $h = 0$) can be calculated using the following equation:

$$D(\text{voxel}_k) = \sum_{h=0}^{N} \widetilde{A}_{\text{voxel}_h} . S(\text{voxel}_k \leftarrow \text{voxel}_h), \quad (2)$$

where $\widetilde{A}_{\text{voxel}_h}$ is the time-integrated activity in the source voxel, h and $S(\text{voxel}_k \leftarrow \text{voxel}_h)$ are the voxel S values that are defined as the mean absorbed dose to a target voxel per radioactivity decay in a source voxel, both of which are contained in an infinite homogenous tissue medium [29].

Tabulations of voxel S values for several voxel dimensions calculated with MC code for a few radionuclides were reported in MIRD pamphlet no. 17. The MIRD formalism using voxel S values is possibly the most accepted and easy to implement method for voxel-based dosimetry that does not require volume integrations of the dose point kernel (DPK) over sources and targets [60]. However, the preclinical voxel S value dataset for different radionuclides at various voxel sizes is not yet available to perform voxel-based dosimetry in small animals using a MIRD schema. Moreover, a voxel S value approach does not consider tissue nonhomogeneity during absorbed dose calculations [29, 30].

Voxel-Based Small Animal Models

Over the past two decades, there have been significant developments in the generation of digital models of mice and rats for the calculation of organ-absorbed doses in preclinical TRT. Among these models, the majority of mouse phantoms are stylized, containing organs with simplified geometries [27, 28, 55]. With advancements in high-resolution tomographic imaging systems (CT and MRI), more anatomically realistic voxel-based models have emerged, either from tomographic images or from digital photographs of mice cryosections [61–64]. Significant differences in absorbed dose results have been reported when stylized and voxel-based models have been used in Monte Carlo simulations [63–65]. Hindorf et al. [55] used stylized mathematical models for mouse dosimetry and observed discrepancies in the calculated S values that led to differences in absorbed dose calculations, particularly for high-energy beta emitters, when the mass, shape, and relative locations of organs within the mouse body were considered. Their results showed that S values could differ as much as 80% from their true value if linear interpolation from S value tables is used to obtain an S value for the specific mass of an organ. They further found that the shape of an organ is not crucial for S value calculation. However, their results showed that the cross-absorbed S value is strongly dependent on geometry and emitted radiation. The new high-quality mesh-type adult reference computational phantoms developed by the International Commission on Radiological Protection (ICRP) include all important source and target tissues for the estimation of effective dose, thereby obviating the need for supplemental organ-specific stylized models [66].

In 2004, Segars et al. developed 4D digital mouse body (MOBY) and rat body (ROBY) phantoms that are based on non-uniform rational b-spline (NURBS) mathematical models to define organ boundaries [67–69]. Several researchers have adopted MOBY phantoms for MC simulations to calculate organ S values for absorbed dose estimation in TRT [17, 23, 24, 70–73]. However, a study performed by Mauxion et al. [23] demonstrated the limitations of using digital mouse models for MC-based absorbed dose calculations. They observed very different dose distributions in some organs when two similar mouse models generated from the same software were used. Kostou et al. [17] and Boutaleb et al. [52] concluded that no specific digital mouse model could be applied for individualized dosimetry in murine studies because small variations in mouse anatomy may significantly affect the absorbed dose results (Fig. 1).

Monte Carlo Radiation Transport Codes

Many MC radiation transport codes, such as MCNPx, EGSnrc, PENELOPE, and Geant4/Geant4 Application for Emission Tomography (GATE), were developed in the last few years to calculate absorbed dose at the voxel level. Following the development of more realistic preclinical voxel-based phantoms, several dosimetry studies have been performed using these MC codes to estimate small animal-specific absorbed fractions (SAFs), organ-level S values, and voxel S values for various diagnostic and therapeutic radionuclides [60–64, 70–73]. EGSnrc [74] and MCNPx [75] have been widely accepted and are considered reference MC codes for dosimetry simulations involving electron-photon transport at low energies down to 1 keV. Bitar et al. calculated S values for various radionuclides, including ^{90}Y and ^{188}Re, for a large number of source-target combinations using the MCNP MC Code in a 30-g mouse model [63]. Xie and Zaidi generated an S values database for various PET radionuclides using MCNPX MC in the MOBY phantom for the assessment of radiation dose to mice [70]. Lanconelli et al. provided a free dataset of voxel S values for therapeutic radionuclides, including ^{177}Lu, at various voxel sizes for TRT dosimetry using DOSXYZnrc code [60].

Recently, the GATE, an MC toolkit [76] based on Geant4 [77], is being used frequently for both clinical and preclinical dosimetry applications. By using Geant4, we can simulate the electromagnetic interactions of photons, electrons, hadrons, and ions with matter down to the electron volt energy scale

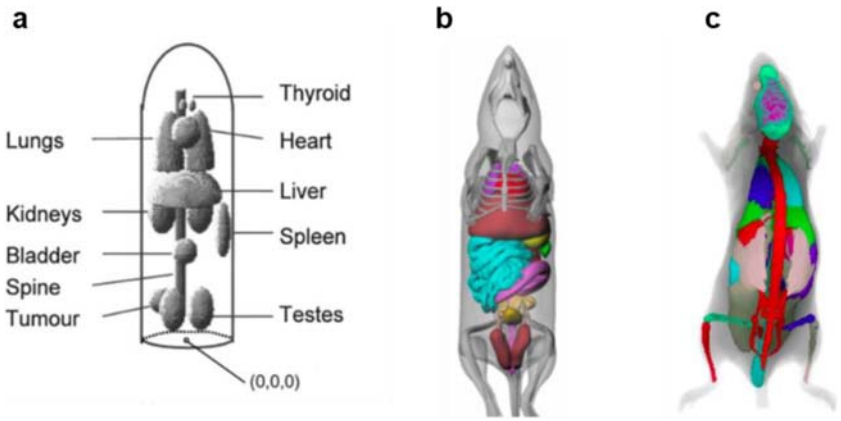

Fig. 1 Examples of mouse models. **a** Stylized (Hindorf et al. 2004). **b** MOBY (Segars et al. 2004). **c** Bitar et al. (2007)

[77, 78]. Various studies have been performed to validate the reliability and accuracy of GATE MC for preclinical dosimetry [17, 23, 72].

Voxel-Based Dosimetry

In TRT, normal tissue toxicity and therapeutic efficacy are of great concern, and there is much less tolerance for inaccuracies in absorbed dose calculations. Therefore, to consider nonuniform activity distributions in organs for accurately calculating absorbed dose, voxel-based dosimetry methods that use DPK [79, 80] or voxel *S* value (VSV) approaches [51] have been suggested. The DPK method of voxel-based dosimetry is limited when compared with the VSV approach because it requires CPU-intensive conversions of spherical coordinates to Cartesian coordinates over the target volumes. The use of the VSV approach is also limited because of the requirement for a VSV database of each radionuclide at various voxel sizes. Moreover, these methods do not incorporate heterogeneity in the organ tissues into the absorbed dose calculations.

Direct MC (DMC) simulation is believed to produce more realistic dose distributions at the voxel level with high precision because it can handle tissue heterogeneity as well as nonuniform source distributions [81–84]. With advancements in 3D imaging modalities and user-friendly MC codes, several groups have developed personalized dosimetry tools for clinical applications, such as 3D Internal Dosimetry (3D-ID) [85], the Royal Marsden Dosimetry Package (RMDP) [86], VoxelDose [87], 3D Radiobiological Dosimetry (3D-RD) [81], Dose Planning Method (DPM) [88], RAYDOSE [89], and VIDA [90]. Recently, Bednarz et al. [65] introduced an MC-based preclinical dosimetry platform, called the Radionuclide Assessment Platform for Internal Dosimetry (RAPID), which is capable of calculating murine-specific 3D dose distributions.

Although DMC simulation has been validated for clinical TRT dosimetry applications, only a small number of preclinical dosimetry studies using DMC simulation have been reported [17, 23, 72, 91–93]. Furthermore, these studies used standard mouse models, such as the MOBY phantom, for MC dosimetry simulations. In recent preclinical dosimetry simulations performed with MOBY phantoms, authors demonstrated that small variations in organ anatomy could significantly impact the dose calculations [17, 52]. Therefore, they suggested that personalized dosimetry might not produce accurate absorbed dose values when a specific murine model is used for preclinical TRT. Using 3D imaging data from individual mice in MC simulations might reduce errors in voxel-based dose calculations arising from the variation in organ anatomies and activity distributions. Gupta et al. [93] evaluated the feasibility of GATE MC simulations for preclinical voxel-based absorbed dose calculations using ^{18}F-FDG PET/CT imaging data of individual normal mice. Because GATE MC simulation considers tissue heterogeneity and nonhomogeneous activity distributions within the mouse body, the voxel-based absorbed doses, as calculated from ^{18}F-FDG PET data in their study, are considered to be more realistic and mouse-specific. From the validation study, it was concluded that the GATE MC simulation toolkit could be applied to murine-specific voxel-based dosimetry in preclinical PRRT to perform tumor absorbed dose calculations more accurately (Fig. 2).

^{177}Lu-Based Preclinical PRRT Dosimetry

Peptide receptor TRT using ^{177}Lu has gained an established role in the preclinical assessment and implementation of clinically relevant diagnostics or therapeutics [94–100]. ^{177}Lu is a theranostic radionuclide having several advantages in performing imaging studies for the evaluation of radiotracer biodistribution as well as for cancer therapy [95]. The lower tissue penetration range and the efficient cross-fire effect of ^{177}Lu may kill small tumors more effectively relative to other theranostic radionuclides [19]. Because of their short range, β-particles emitted from ^{177}Lu traverse several cells (10–1000), causing the destruction of multiple cells in the vicinity

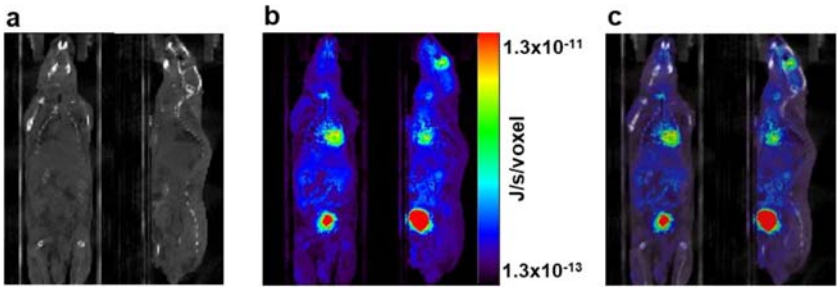

Fig. 2 Voxel-based dosimetry based on direct Monte Carlo (DMC) simulation. **a** CT image of a mouse used for GATE MC simulation. **b** Output of simulation or dose map. **c** Dose map overlaid on the CT image. Coronal (left) and sagittal (right) views of the images are shown respectively in the figure. Gupta et al. [93]

of the cells that accumulate the radiotracer [94, 95]. This effect is known as the "cross-fire effect" and is crucial for ensuring that a sufficient dose is delivered to each cell and for improving the homogeneity of tumor dose during cancer therapy [96].

Quantitative ^{177}Lu-SPECT Imaging

The absorbed dose calculations for PRRT are based on residence times obtained from serial quantitative SPECT/CT images acquired at multiple time points. Hence, the quantitative accuracy during ^{177}Lu-SPECT imaging is essential for reliably assessing tumor uptake and tumor-to-normal tissue ratios necessary to perform personalized dosimetry [101–103]. Accurate image quantitation in small animal SPECT is always challenging due to the limitations in the instrumentation and imaging process; therefore, it is important to evaluate performance parameters of preclinical SPECT systems used for theranostic radionuclides during pre- and post-therapy dosimetry studies [103, 104]. Mezzenga et al. [103] evaluated the quantitative accuracy of ^{177}Lu SPECT imaging for both small and large objects using cylindrical homogeneous reference geometry. The authors investigated the relationship between 3D-OSEM algorithm, object size, and coefficient of variation to demonstrate that ^{177}Lu SPECT is suitable for activity quantification in small volumes.

Gupta et al. [47] performed several phantom studies to evaluate the quantitative accuracy and performance parameters (recovery coefficient, uniformity, spatial resolution, and sensitivity and calibration factor) of a multi-pinhole SPECT/CT system for ^{177}Lu imaging. They investigated the relationship between activity recovery and image uniformity at different iteration numbers during iterative image reconstructions (3D-OSEM). In addition, the performance parameters of the SPECT camera measured for ^{177}Lu were compared with those of ^{99m}Tc. The quantitative accuracy achieved in their study plays an important role in activity quantification when performing ^{177}Lu-SPECT imaging in mice for personalized dosimetry.

Murine-Specific ^{177}Lu-Dosimetry

The activity administered during radionuclide therapy is generally determined conservatively to avoid potential toxicity; however, this approach may result in sub-therapeutic treatments, causing cancer recurrence [105]. In clinical trials, ^{177}Lu therapy delivered at a fixed level of activity shows promising results in terms of treatment outcome. Nevertheless, several studies showed that pretherapy patient-specific dosimetry plays an important role in treatment planning during TRT of various cancers to improve the probability of tumor control and reduce normal tissue toxicity [106–108]. This concept may also apply to preclinical TRT using ^{177}Lu-labeled radiopharmaceuticals, and voxel-based dosimetry is essential to achieve more accurate dosimetry results for the interpretation of the radiobiological response. However, only a few voxel-based dosimetry studies of preclinical ^{177}Lu TRT that are based on MC simulations of digital murine models have been reported [109–112].

Vilchis-Juarez et al. [49] performed voxel-based dosimetry using MC codes and compared the absorbed doses in kidneys and tumors to evaluate the therapeutic response of ^{177}Lu-AuNP-RGD in athymic nude mice bearing $\alpha(v)\beta(3)$-integrin-positive C6 gliomas. Haller et al. [109] investigated the therapeutic anti-tumor effects and radiation-induced nephrotoxicity of ^{177}Lu-cm09 and ^{177}Lu-EC0800 in KB tumor-bearing mice by estimating equivalent absorbed doses using PENELOPE MC simulation code. Kuo et al. [110] synthesized ^{177}Lu-HTK01169, a close analog of 177Lu-PSMA-617, and performed biodistribution and dosimetry studies in mice bearing PSMA-expressing LNCaP tumor xenografts using SPECT/CT imaging and OLINDA software v.2.0. Timmermand et al. [111] performed whole-body and small-scale tumor dosimetry of ^{177}Lu-labeled hu11B6 in an LNCaP tumor-bearing mice model using mouse-specific S-factors calculated with the MCNP6 MC package. Gupta et al. [112] recently synthesized ^{177}Lu-IONPs-Folate for preclinical targeted imaging and therapy of folate receptor-positive cancer and calculated voxel-based organ absorbed doses using SPECT/CT images of normal and KB tumor-bearing mice

using a GATE MC simulation. They compared kidney- and tumor-absorbed doses at the voxel level obtained with ^{177}Lu-IONPs-Folate with those obtained with ^{177}Lu-labeled folic acid without IONPs (^{177}Lu-Folate) and ^{177}Lu-IONPs only. They found that the voxel-based absorbed dose to kidneys from ^{177}Lu-IONPs-Folate was almost half relative to that obtained with ^{177}Lu-Folate only. The tumor dose at the voxel level received from ^{177}Lu-IONPs-Folate was the highest when compared with those of ^{177}Lu-Folate and ^{177}Lu-IONP. Their study suggested that voxel-based dosimetry using MC simulations is reliable and potentially more accurate for ^{177}Lu-IONPs-Folate therapy of folate receptor-positive cancers on a personalized basis (Figs. 3 and 4).

Fast Voxel-Based Dosimetry for Preclinical TRT

Although MC simulation is currently the most accurate method for voxel-based absorbed dose calculations, it is time-consuming, computationally demanding, and often impractical to carry out in practice [113, 114]. Therefore, several groups have proposed fast, voxel-based dosimetry methods based on DPK, multiple VSV, and semi-Monte Carlo (sMC) techniques that have been shown to overcome the limitations associated with the DMC method in clinical dosimetry [115–119].

Hippeläinen et al. [117] proposed a fast sMC code for ^{177}Lu PRRT dose calculations, which was based on the assumption of local electron absorption and fast photon MC simulations. Since the simulations of electrons are the most demanding part of MC simulations, electron absorption assumptions accelerate the absorbed dose calculations dramatically. Their results suggested that there is no need of electron simulation for ^{177}Lu absorption calculations when SPECT imaging system is used. Therefore, when the sMC method is applied with its local electron absorption assumption, voxel-based dosimetry, especially for ^{177}Lu PRRT, can be successfully performed with four SPECT/CT scans in 4 to 5 min. However, this fast sMC dosimetry method is only applicable to low-energy electrons emitted from ^{177}Lu because this method has not yet been validated for radioisotopes emitting high-energy electrons, such as ^{90}Y or ^{131}I.

Recently, Lee et al. [119] proposed a fast and new method for voxel-based absorbed dose calculations using multiple VSVs that considers both nonhomogeneous activities and heterogeneous media. They applied MC simulation to acquire multiple VSVs with various densities and utilized them to acquire dose maps using CT-based segmentation. The authors successfully implemented the proposed dosimetry approach on digital phantom and whole-body dynamic ^{68}Ga-PET images of patients. The results obtained were comparable to those with the DMC technique and had the advantage of a significantly reduced dose-computation time. Because their proposed dosimetry method was fast and more accurate and generated dose maps at the whole-body level, it can be applied for personalized dosimetry in TRT. Most recently, Lee et al. [120] proposed a voxel-based dosimetry approach using a

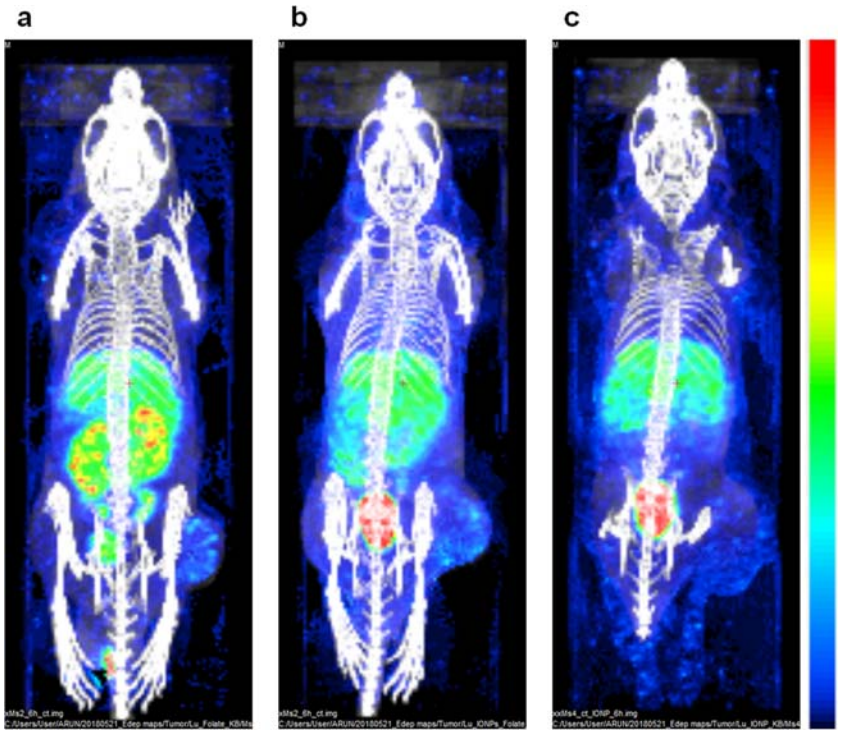

Fig. 3 Maximum intensity projection images showing dose maps overlaid on the CT images of ^{177}Lu-Folate (**a**), ^{177}Lu-IONPs-Folate (**b**), and ^{177}Lu-IONPs (**c**) obtained with GATE MC simulations of SPECT/CT of KB tumor-bearing mice acquired at 6 h post-injection. Energy deposited in the tumor at the voxel level was the highest from ^{177}Lu-IONPs-Folate compared with those from ^{177}Lu-Folate and ^{177}Lu-IONPs. Gupta et al. [112]

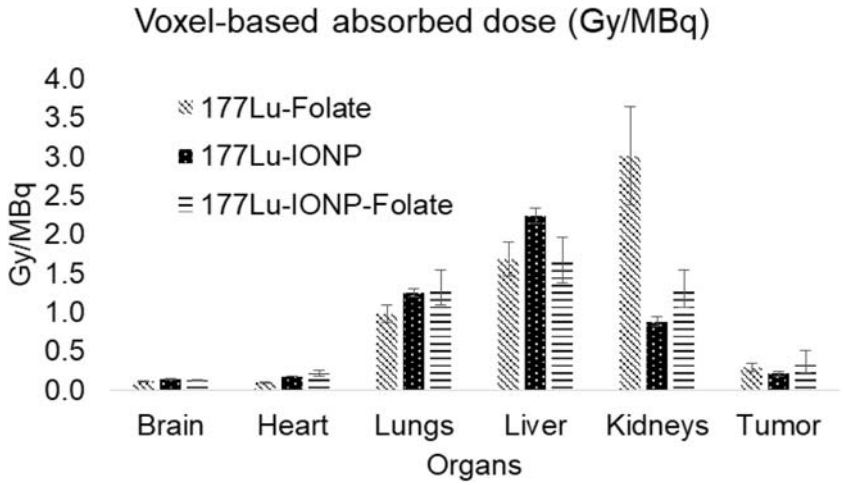

Fig. 4 Voxel-based absorbed doses in organs and tumor (mean ± SD) calculated by GATE MC from ^{177}Lu-Folate, ^{177}Lu-IONPs, and ^{177}Lu-IONPs-Folate in KB tumor-bearing mice. Gupta et al. [112]

deep convolutional neural network (CNN) to overcome the limitations of the DMC method. Their CNN-based personalized dosimetry approach produced results comparable to that of DMC simulation, but with significantly lower computation time. This novel method appears to be more advanced and fast compared to traditional dosimetry methods because new deep learning methods routinely outperform conventional signal and image analysis techniques in multiple medical engineering fields [121–126].

Extrapolation of Data from Mouse to Human

Because it is possible to translate preclinical dosimetry data to a clinical setting, preclinical research using small animals has been used with increasing frequency to develop novel theranostic agents and to establish a relationship between absorbed dose and biological effects during preclinical TRT [23, 65]. Because very few patient-specific dosimetry studies are available in clinical theranostics, the ability to extrapolate data from mouse to human for the assessment of absorbed dose in the critical organs from novel theranostic radiopharmaceuticals is essential.

Various authors reporting preclinical TRT studies have presented methods to extrapolate dosimetry values from preclinical to clinical settings for the evaluation of radiation-induced organ toxicity and treatment response during clinical trials of new radiopharmaceuticals [127–132]. However, several assumptions and technical complexities arise during the measurement of radiotracer biodistribution and the extrapolation of data from the animal model to humans [132]. In addition, predetermined absorbed dose values in humans that are derived from animal dosimetry data have not been validated. Stabin et al. presented a method for extrapolating biodistribution uptake data from mice to human for dosimetry calculations that was based on two options for interspecies scaling [57, 133].

During the extrapolation of data from mouse to human, several factors have been reported to cause discrepancies between mouse- and human-derived organ-absorbed doses. The variation in size and anatomy, interspecies differences in pharmacokinetics, and methodological differences in biodistribution measurements were considered to be the main factors responsible for such discrepancies. Repetto-Llamazares et al. [131] calculated the absorbed dose in mice from ^{177}Lu-tetraxetan-tetulomab and ^{177}Lu-tetraxetan-rituximab and successfully extrapolated the dosimetry data to a human absorbed dose. Sakata et al. [132] observed that the extrapolation of data from mouse to human is roughly acceptable; however, the differences in the proportions of organ mass to total body mass cause inconsistencies in the predicted dosimetry for human subjects. Hence, dosimetry studies in humans to assess radiation risk and dose-response relationships are essential for clinical trials of newly developed theranostic radiopharmaceuticals.

Future Perspective

Due to the increasing use of preclinical TRT studies for the development of novel theranostic agents, several studies have been performed to accurately estimate absorbed doses to mice at the voxel level using reference mouse phantoms and MC simulations. The fast voxel-level dosimetry approaches developed for clinical TRT studies could also be validated for preclinical voxel-based dosimetry to reduce computation time when longitudinal SPECT/CT imaging of mice is performed. Accurate absorbed dose calculations at the voxel level are necessary to interpret the radiobiological response during personalized therapy of small animals. In EBRT, the methods for evaluating radiobiological effects are well established; however, a dedicated dosimetry method needs to be developed for TRT for radiobiological modeling.

Three-dimensional imaging-based dosimetry applications that have already been applied [85–90] to patient-specific

dosimetry should also be upgraded and validated for voxel-based absorbed dose calculations in preclinical TRT. Bednarz et al. [65] recently proposed a preclinical voxel-based dosimetry platform, called RAPID, that is capable of calculating murine-specific 3D dose distributions from theranostic agents used for imaging and therapy. In addition to absorbed doses, dose-volume histograms (DVH) can also be calculated using RAPID to assess the absorbed dose heterogeneity in the tumors. Furthermore, RAPID is currently being upgraded to calculate the biologically effective dose (BED) at the voxel level, which will be useful for radiobiological interpretation and modeling of the dose distribution for response assessment in preclinical TRT. The use of real 3D imaging data of mouse instead of the standard mouse model for MC simulations could further reduce errors in mouse-specific absorbed dose calculations because this approach considers the individualized organ anatomy and activity distributions of each mouse during dosimetry simulations.

Conclusion

The estimation of absorbed doses from radionuclides has become essential for preclinical studies that use small animals because these estimations are essential to the development of novel theranostic agents. The development of more realistic voxel-based preclinical phantoms and user-friendly advanced MC codes has made more accurate absorbed dose calculations at the voxel level possible for preclinical theranostics. Although voxel-based dosimetry using MC simulation is currently the most accurate technique, it is cumbersome and time-consuming. Fast voxel-based absorbed dose calculations based on DPK, multiple VSV, and sMC techniques have been shown to overcome limitations associated with the DMC method in clinical dosimetry. The extension of such methods to preclinical TRT dosimetry would be very useful for optimizing the computation time required to perform absorbed dose calculations. In this review article, we discussed the present scenario of preclinical imaging and dosimetry at the voxel level that is performed using various voxel-based murine models and MC radiation transport codes. We also presented the limitations of various voxel-based dosimetry methods and gave an overview of the possibilities for fast voxel-based absorbed dose calculations in preclinical theranostics.

Funding Information This work was supported by grants from National Research Foundation of Korea (NRF) funded by the Korean Ministry of Science, ICT and Future Planning (grant no. NRF-2016R1A2B3014645).

Compliance with Ethical Standards

Conflict of Interest Arun Gupta, Min Sun Lee, Joong Hyun Kim, Dong Soo Lee, and Jae Sung Lee declare that they have no conflict of interest.

Ethical Statement All procedures performed in studies involving animals were in accordance with the ethical standards of Seoul National University, College of Medicine, Seoul, South Korea.

Informed Consent For this type of study, informed consent is not required.

References

1. Lewis JS, Achilefu S, Garbow JR, Laforest R, Welch MJ. Small animal imaging: current technology and perspectives for oncological imaging. Eur J Cancer. 2002;38:2173–88.
2. Grassi R, Cavaliere C, Cozzolino S, Mansi L, Cirillo S, Tedeschi G, et al. Small animal imaging facility: new perspectives for the radiologist. Radiol Med. 2009;114:152–67.
3. Dash A, Chakraborty S, Pillai MRA, Knapp FF. Peptide receptor radionuclide therapy: an overview. Cancer Biother Radiopharm. 2015;30:47–71.
4. Flux G, Bardies M, Monsieurs M, Savolainen S, Strand SE, Lassmann M. The impact of PET and SPECT on dosimetry for targeted radionuclide therapy. Z Med Phys. 2006;16:47–59.
5. de Jong M, Breeman WA, Bernard BF, Bakker WH, Schaar M, van Gameren A, et al. [177Lu-DOTA0,Tyr3]octreotate for somatostatin receptor-targeted radionuclide therapy. Int J Cancer. 2001;92:628–33.
6. Pool SE, Krenning EP, Koning GA, van Eijck CH, Teunissen JJ, Kam B, et al. Preclinical and clinical studies of peptide receptor radionuclide therapy. Semin Nucl Med. 2010;40(3):209–18.
7. Paganelli G, Sansovini M, Ambrosetti A, Severi S, Monti M, Scarpi E, et al. ^{177}Lu-Dota-octreotate radionuclide therapy of advanced gastrointestinal neuroendocrine tumors: results from a phase II study. Eur J Nucl Med Mol Imaging. 2014;41:1845–51.
8. Kost SD. Patient-specific dosimetry for targeted radionuclide therapy using deformable anthropomorphic phantoms: Vanderbilt University; 2015.
9. Ersahin D, Doddamane I, Cheng D. Targeted radionuclide therapy. Cancers. 2011;3:3838.
10. Giblin MF, Veerendra B, Smith CJ. Radiometallation of receptor-specific peptides for diagnosis and treatment of human cancer. In Vivo. 2005;19:9–29.
11. de Jong M, Breeman WA, Kwekkeboom DJ, Valkema R, Krenning EP. Tumor imaging and therapy using radiolabeled somatostatin analogues. Acc Chem Res. 2009;42:873–80.
12. Müller C, Struthers H, Winiger C, Zhernosekov K, Schibli R. DOTA conjugate with an albumin-binding entity enables the first folic acid–targeted ^{177}Lu-radionuclide tumor therapy in mice. J Nucl Med. 2013;54:124–31.
13. Birn H, Spiegelstein O, Christensen EI, Finnell RH. Renal tubular reabsorption of folate mediated by folate binding protein 1. J Am Soc Nephrol. 2005;16:608–15.
14. Holm J, Hansen SI, Høier-Madsen M, Bostad L. A high-affinity folate binding protein in proximal tubule cells of human kidney. Kidney Int. 1992;41:50–5.
15. Sandoval RM, Kennedy MD, Low PS, Molitoris BA. Uptake and trafficking of fluorescent conjugates of folic acid in intact kidney determined using intravital two-photon microscopy. Am J Phys Cell Phys. 2004;287:C517.
16. Kolbert KS, Watson T, Matei C, Xu S, Koutcher JA, Sgouros G. Murine S factors for liver, spleen, and kidney. J Nucl Med. 2003;44:784–91.
17. Theodora K, Panagiotis P, George L, George CK. A preclinical simulated dataset of S -values and investigation of the impact of

rescaled organ masses using the MOBY phantom. Phys Med Biol. 2016;61:2333.
18. Strigari L, Konijnenberg M, Chiesa C, Bardies M, Du Y, Gleisner KS, et al. The evidence base for the use of internal dosimetry in the clinical practice of molecular radiotherapy. Eur J Nucl Med Mol Imaging. 2014;41:1976–88.
19. Cremonesi M, Ferrari M, Bodei L, Tosi G, Paganelli G. Dosimetry in peptide radionuclide receptor therapy: a review. J Nucl Med. 2006;47:1467–75.
20. Cremonesi M, Ferrari M, Di Dia A, Botta F, De Cicco C, Bodei L, et al. Recent issues on dosimetry and radiobiology for peptide receptor radionuclide therapy. Q J Nucl Med Mol Imaging. 2011;55:155–67.
21. Stabin MG, Brill AB. State of the art in nuclear medicine dose assessment. Semin Nucl Med. 2008;38:308–20.
22. Funk T, Sun M, Hasegawa BH. Radiation dose estimate in small animal SPECT and PET. Med Phys. 2004;31:2680–6.
23. Mauxion T, Barbet J, Suhard J, Pouget J-P, Poirot M, Bardiès M. Improved realism of hybrid mouse models may not be sufficient to generate reference dosimetric data. Med Phys. 2013;40:052501.
24. Larsson E, Ljungberg M, Strand S-E, Jönsson B-A. Monte Carlo calculations of absorbed doses in tumours using a modified MOBY mouse phantom for pre-clinical dosimetry studies. Acta Oncol. 2011;50:973–80.
25. Dewaraja YK, Wilderman SJ, Ljungberg M, Koral KF, Zasadny K, Kaminiski MS. Accurate dosimetry in (131)I radionuclide therapy using patient-specific, 3-dimensional methods for SPECT reconstruction and absorbed dose calculation. J Nucl Med. 2005;46:840–9.
26. Dewaraja YK, Frey EC, Sgouros G, Brill AB, Roberson P, Zanzonico PB, et al. MIRD pamphlet no. 23: quantitative SPECT for patient-specific 3-dimensional dosimetry in internal radionuclide therapy. J Nucl Med. 2012;53:1310–25.
27. Flynn AA, Green AJ, Pedley RB, Boxer GM, Boden R, Begent RHJ. A mouse model for calculating the absorbed beta-particle dose from 131I- and 90Y-labeled immunoconjugates, including a method for dealing with heterogeneity in kidney and tumor. Radiat Res. 2001;156:28–35.
28. Edmond Hui T, Fisher DR, Kuhn JA, Williams LE, Nourigat C, Badger CC, et al. A mouse model for calculating cross-organ beta doses from yttrium-90-labeled immunoconjugates. Cancer. 1994;73:951–7.
29. Bolch WE, Bouchet LG, Robertson JS, Wessels BW, et al. MIRD pamphlet no, 17: the dosimetry of nonuniform activity distributions–radionuclide S-values at the voxel level. J Nucl Med. 1999;40:11S–36S.
30. Bolch WE, Eckerman KF, Sgouros G, Thomas SR. MIRD pamphlet no. 21: a generalized Schema for radiopharmaceutical dosimetry—standardization of nomenclature. J Nucl Med. 2009;50:477–84.
31. Sofou S. Radionuclide carriers for targeting of cancer. Int J Nanomedicine. 2008;3:181–99.
32. Kassis AI. Therapeutic radionuclides: biophysical and radiobiologic principles. Semin Nucl Med. 2008;38:358–66.
33. Lee DS, Im H-J, Lee Y-S. Radionanomedicine: widened perspectives of molecular theragnosis. Nanomedicine. 2015;11:795–810.
34. Tolmachev V, Orlova A, Pehrson R, Galli J, Baastrup B, Andersson K, et al. Radionuclide therapy of HER2-positive microxenografts using a ^{177}Lu-labeled HER2-specific Affibody molecule. Cancer Res. 2007;67:2773.
35. Franc BL, Acton PD, Mari C, Hasegawa BH. Small-animal SPECT and SPECT/CT: important tools for preclinical investigation. J Nucl Med. 2008;49:1651–63.
36. Habraken JBA, de Bruin K, Shehata M, Booij J, Bennink R, van Eck Smit BLF, et al. Evaluation of high-resolution pinhole SPECT using a small rotating animal. J Nucl Med. 2001;42:1863–9.
37. Blankenberg FG, Strauss HW. Nuclear medicine applications in molecular imaging. J Magn Reson Imaging. 2002;16:352–61.
38. Schäfers KP. Imaging small animals with positron emission tomography. Nuklearmedizin. 2003;42:86–9.
39. Cheng D, Wang Y, Liu X, Pretorius PH, Liang M, Rusckowski M, et al. Comparison of ^{18}F PET and ^{99m}Tc SPECT imaging in phantoms and in tumored mice. Bioconjug Chem. 2010;21:1565–70.
40. Del Guerra A, Belcari N. State-of-the-art of PET, SPECT and CT for small animal imaging. Nucl Instrum Methods Phys Res A. 2007;583:119–24.
41. Andrew BH, Benjamin LF, Grant TG, Bruce HH. Assessment of the sources of error affecting the quantitative accuracy of SPECT imaging in small animals. Phys Med Biol. 2008;53:2233.
42. Freek JB, Brendan V. Design and simulation of a high-resolution stationary SPECT system for small animals. Phys Med Biol. 2004;49:4579.
43. Schramm NU, Ebel G, Engeland U, Schurrat T, Behe M, Behr TM. High-resolution SPECT using multipinhole collimation. IEEE Trans Nucl Sci. 2003;50:315–20.
44. Schramm N, Hoppin J, Lackas C, Gershman B, Norenberg J, de Jong M. Improving resolution, sensitivity and applications for the NanoSPECT/CT: a high-performance SPECT/CT imager for small-animal research. J Nucl Med. 2007;48:436P.
45. Frank PD. Design and performance of a multi-pinhole collimation device for small animal imaging with clinical SPECT and SPECT–CT scanners. Phys Med Biol. 2008;53:4185.
46. Finucane CM, Murray I, Sosabowski JK, Foster JM, Mather SJ. Quantitative accuracy of low-count SPECT imaging in phantom and in vivo mouse studies. Int J Mol Imaging. 2011;2011:8.
47. Gupta A, Kim KY, Hwang D, Lee MS, Lee DS, Lee JS. Performance evaluation and quantitative accuracy of multipinhole NanoSPECT/CT scanner for theranostic Lu-177 imaging. J Korean Phys Soc. 2018;72:1379–86.
48. Li T, Ao ECI, Lambert B, Brans B, Vandenberghe S, Mok GSP. Quantitative imaging for targeted radionuclide therapy dosimetry - technical review. Theranostics. 2017;7:4551–65.
49. Vilchis-Juárez A, Ferro-Flores G, Santos-Cuevas C, Morales-Avila E, Ocampo-García B, Díaz-Nieto L, et al. Molecular targeting radiotherapy with cyclo-RGDfK(C) peptides conjugated to 177Lu-labeled gold nanoparticles in tumor-bearing mice. J Biomed Nanotechnol. 2014;10:393–404.
50. Loevinger R, Budinger TF, Watson EE, Society of Nuclear Medicine. Medical internal radiation dose C. MIRD Primer for Absorbed Dose Calculations: Society of Nuclear Medicine; 1988.
51. Stabin MG, Eckerman KF, Bolch WE, Bouchet LG, Patton PW. Evolution and status of bone and marrow dose models. Cancer Biother Radiopharm. 2002;17:427–33.
52. Boutaleb S, Pouget JP, Hindorf C, Pelegrin A, Barbet J, Kotzki PO, et al. Impact of mouse model on preclinical dosimetry in targeted radionuclide therapy. Proc IEEE. 2009;97:2076–85.
53. Muthuswamy MS, Roberson PL, Buchsbaum DJ. A mouse bone marrow dosimetry model. J Nucl Med. 1998;39:1243–7.
54. Miller WH, Hartmann-Siantar C, Fisher D, Descalle M-A, Daly T, Lehmann J, et al. Evaluation of beta-absorbed fractions in a mouse model for ^{90}Y, ^{188}Re, ^{166}Ho, ^{149}Pm, ^{64}Cu, and ^{177}Lu radionuclides. Cancer Biother Radiopharm. 2005;20:436–49.
55. Hindorf C, Ljungberg M, Strand S-E. Evaluation of parameters influencing S values in mouse dosimetry. J Nucl Med. 2004;45:1960–5.
56. Stabin MG. MIRDOSE: personal computer software for internal dose assessment in nuclear medicine. J Nucl Med. 1996;37:538–46.
57. Stabin MG, Sparks RB, Crowe E. OLINDA/EXM: the second-generation personal computer software for internal dose assessment in nuclear medicine. J Nucl Med. 2005;46:1023–7.

58. Stabin MG, Konijnenberg MW. Re-evaluation of absorbed fractions for photons and electrons in spheres of various sizes. J Nucl Med. 2000;41:149–60.
59. Parach AA, Rajabi H, Askari MA. Assessment of MIRD data for internal dosimetry using the GATE Monte Carlo code. Radiat Environ Biophys. 2011;50:441–50.
60. Lanconelli N, Pacilio M, Meo SL, Botta F, Dia AD, Aroche LAT, et al. A free database of radionuclide voxel S values for the dosimetry of nonuniform activity distributions. Phys Med Biol. 2012;57:517–33.
61. Stabin MG, Peterson TE, Holburn GE, Emmons MA. Voxel-based mouse and rat models for internal dose calculations. J Nucl Med. 2006;47:655–9.
62. Dogdas B, Stout D, Chatziioannou, Leahy RM. Digimouse: a 3D whole body mouse atlas from CT and cryosection data. Phys Med Biol. 2007;52:577–87.
63. Bitar A, Lisbona A, Bardiès M. S-factor calculations for mouse models using Monte-Carlo simulations. Q J Nucl Med Mol Imaging. 2007;51:343–51.
64. Bitar A, Lisbona A, Thedrez P, Sai Maurel C, Le Forestier D, Barbet J, et al. A voxel-based mouse for internal dose calculations using Monte Carlo simulations (MCNP). Phys Med Biol. 2007;52:1013–25.
65. Bednarz B, Grudzinski J, Marsh I, Besemer A, Baiu D, Weichert J, et al. Murine-specific internal dosimetry for preclinical investigations of imaging and therapeutic agents. Health Phys. 2018;114:450–9.
66. Kim CH, Yeom YS, Nguyen TT, Han MC, Choi C, Lee H, Han H, Shin B, Lee J-K, Kim HS, Zankl M, Petoussi-Henss N, Bolch WE, Lee C, Chung BS, Qiu R, Eckerman K. New mesh-type phantoms and their dosimetric applications, including emergencies. Ann ICRP. 2018;47(3–4):45–62.
67. Segars WP, Tsui BMW, Frey EC, Johnson GA, Berr SS. Development of a 4-D digital mouse phantom for molecular imaging research. Mol Imaging Biol. 2004;6:149–59.
68. Segars W, Tsui B. 4D MOBY and NCAT phantoms for medical imaging simulation of mice and men. J Nucl Med. 2007;48:203P.
69. Segars WP, Sturgeon G, Mendonca S, Grimes J, Tsui BM. 4D XCAT phantom for multimodality imaging research. Med Phys. 2010;37:4902–15.
70. Xie T, Zaidi H. Monte Carlo-based evaluation of S-values in mouse models for positron-emitting radionuclides. Phys Med Biol. 2013;58:169–82.
71. Larsson E, Strand S-E, Ljungberg M, Jönsson B-A. Mouse S-factors based on Monte Carlo simulations in the anatomical realistic Moby phantom for internal dosimetry. Cancer Biother Radiopharm. 2007;22:438–42.
72. Taschereau R, Chatziioannou AF. Monte Carlo simulations of absorbed dose in a mouse phantom from 18-fluorine compounds. Med Phys. 2007;34:1026–36.
73. Keenan MA, Stabin MG, Segars WP, Fernald MJ. RADAR realistic animal model series for dose assessment. J Nucl Med. 2010;51:471–6.
74. Buckley LA, Kawrakow I, Rogers DW. An EGSnrc investigation of cavity theory for ion chambers measuring air kerma. Med Phys. 2003;30:1211–8.
75. Hendricks JS, Adam KJ, Booth TE, Briesmeister JF, Carter LL, Cox LJ, et al. Present and future capabilities of MCNP. Appl Radiat Isot. 2000;53:857–61.
76. Jan S, Santin G, Strul D, Staelens S, Assié K, Autret D, et al. GATE: a simulation toolkit for PET and SPECT. Phys Med Biol. 2004;49:4543.
77. Allison J, Amako K, Apostolakis JE, Araujo HA, Dubois PA, Asai MA, et al. Geant4 developments and applications. IEEE Trans Nucl Sci. 2006;53:270–8.
78. Sarrut D, Bardiès M, Boussion N, Freud N, Jan S, Létang JM, et al. A review of the use and potential of the GATE Monte Carlo simulation code for radiation therapy and dosimetry applications. Med Phys. 2014;41:064301.
79. Berger MJ. Distribution of absorbed dose around point sources of electrons and beta particles in water and other media. Washington: National Bureau of Standards; 1971.
80. Seltzer SM. Electron-photon Monte Carlo calculations: the ETRAN code. Int J Rad Appl Instrum A. 1991;42:917–41.
81. Prideaux AR, Song H, Hobbs RF, He B, Frey EC, Ladenson PW, et al. Three-dimensional radiobiologic dosimetry: application of radiobiologic modeling to patient-specific 3-dimensional imaging-based internal dosimetry. J Nucl Med. 2007;48:1008–16.
82. Sgouros G, Frey E, Wahl R, He B, Prideaux A, Hobbs R. Three-dimensional imaging-based radiobiological dosimetry. Semin Nucl Med. 2008;38:321–34.
83. Dewaraja YK, Schipper MJ, Roberson PL, Wilderman SJ, Amro H, Regan DD, et al. 131I-tositumomab radioimmunotherapy: initial tumor dose-response results using 3-dimensional dosimetry including radiobiologic modeling. J Nucl Med. 2010;51:1155–62.
84. Hobbs RF, Wahl RL, Lodge MA, Javadi MS, Cho SY, Chien DT, et al. 124I PET-based 3D-RD dosimetry for a pediatric thyroid cancer patient: real-time treatment planning and methodologic comparison. J Nucl Med. 2009;50:1844–7.
85. Kolbert KS, Sgouros G, Scott AM, Bronstein JE, Malane RA, Zhang J, et al. Implementation and evaluation of patient-specific three-dimensional internal dosimetry. J Nucl Med. 1997;38:301–7.
86. Guy MJ, Flux GD, Papavasileiou P, Flower MA, Ott RJ. RMDP: a dedicated package for ^{131}I SPECT quantification, registration and patient-specific dosimetry. Cancer Biother Radiopharm. 2003;18:61–9.
87. Gardin I, Bouchet LG, Assié K, Caron J, Lisbona A, Ferrer L, et al. Voxeldose: a computer program for 3-D dose calculation in therapeutic nuclear medicine. Cancer Biother Radiopharm. 2003;18:109–15.
88. Wilderman S, Dewaraja Y. Method for fast CT/SPECT-based 3D Monte Carlo absorbed dose computations in internal emitter therapy. IEEE Trans Nucl Sci. 2007;54:146–51.
89. Marcatili S, Pettinato C, Daniels S, Lewis G, Edwards P, Fanti S, et al. Development and validation of RAYDOSE: a Geant4-based application for molecular radiotherapy. Phys Med Biol. 2013;58:2491.
90. Kost SD, Dewaraja YK, Abramson RG, Stabin MG. VIDA: a voxel-based dosimetry method for targeted radionuclide therapy using Geant4. Cancer Biother Radiopharm. 2015;30:16–26.
91. Jan S, Benoit D, Becheva E, Carlier T, Cassol F, Descourt P, et al. GATE V6: a major enhancement of the GATE simulation platform enabling modelling of CT and radiotherapy. Phys Med Biol. 2011;56:881.
92. Perrot Y, Degoul F, Auzeloux P, Bonnet M, Cachin F, Chezal JM, et al. Internal dosimetry through GATE simulations of preclinical radiotherapy using a melanin-targeting ligand. Phys Med Biol. 2014;59:2183.
93. Gupta A, Lee MS, Kim JH, Park S, Park HS, Kim SE, et al. Preclinical voxel-based dosimetry through GATE Monte Carlo simulation using PET/CT imaging of mice. Phys Med Biol. 2019;64:095007.
94. Brechbiel MW. Targeted alpha-therapy: past, present, future? Dalton Trans. 2007;43:4918–28.
95. Haberkorn U, Giesel F, Morgenstern A, Kratochwil C. The future of radioligand therapy: α, β, or both? J Nucl Med. 2017;58:1017–8.
96. Milenic DE, Brady ED, Brechbiel MW. Antibody-targeted radiation cancer therapy. Nat Rev Drug Discov. 2004;3:488–99.

97. Mendoza-Nava H, Ferro-Flores G, Ramirez FD, Ocampo-Garcia B, Santos-Cuevas C, Aranda-Lara L, et al. ^{177}Lu-dendrimer conjugated to folate and bombesin with gold nanoparticles in the dendritic cavity: a potential theranostic radiopharmaceutical. J Nanomater. 2016;2016:11.
98. Kim K, Kim S-J. Lu-177-based peptide receptor radionuclide therapy for advanced neuroendocrine tumors. Nucl Med Mol Imaging. 2018;52:208–15.
99. Lee S, Xie J, Chen X. Peptide-based probes for targeted molecular imaging. Biochemistry. 2010;49:1364–76.
100. Pratt EC, Shaffer TM, Grimm J. Nanoparticles and radiotracers: advances toward radionanomedicine. Wiley Interdiscip Rev Nanomed Nanobiotechnol. 2016;8:872–90.
101. Ritt P, Vija H, Hornegger J, Kuwert T. Absolute quantification in SPECT. Eur J Nucl Med Mol Imaging. 2011;38:S69–77.
102. Sgouros G, Hobbs RF. Dosimetry for radiopharmaceutical therapy. Semin Nucl Med. 2014;44:172–8.
103. Mezzenga E, D'Errico V, D'Arienzo M, Strigari L, Panagiota K, Matteucci F, et al. Quantitative accuracy of 177Lu SPECT imaging for molecular radiotherapy. PLoS One. 2017;12:e0182888.
104. Hong KJ, Choi Y, Lee SC, Lee SY, Song TY, Min BJ, et al. A compact SPECT/CT system for small animal imaging. IEEE Trans Nucl Sci. 2006;53:2601–4.
105. Stabin MG. Update: the case for patient-specific dosimetry in radionuclide therapy. Cancer Biother Radiopharm. 2008;23:273–84.
106. Ilan E, Sandström M, Wassberg C, Sundin A, Garske-Román U, Eriksson B, et al. Dose response of pancreatic neuroendocrine tumors treated with peptide receptor radionuclide therapy using 177Lu-DOTATATE. J Nucl Med. 2015;56:177–82.
107. Agostinelli S, Allison J, Amako K, Apostolakis J, Araujo H, Arce P, et al. Geant4—a simulation toolkit. Nucl Instrum Methods Phys Res A. 2003;506:250–303.
108. Shcherbinin S, Piwowarska-Bilska H, Celler A, Birkenfeld B. Quantitative SPECT/CT reconstruction for 177Lu and 177Lu/90Y targeted radionuclide therapies. Phys Med Biol. 2012;57:5733.
109. Haller S, Reber J, Brandt S, Bernhardt P, Groehn V, Schibli R, et al. Folate receptor-targeted radionuclide therapy: preclinical investigation of anti-tumor effects and potential radionephropathy. Nucl Med Biol. 2015;42:770–9.
110. Kuo HT, Merkens H, Zhang Z, Uribe CF, Lau J, Zhang C, et al. Enhancing treatment efficacy of 177Lu-PSMA-617 with the conjugation of an albumin-binding motif: preclinical dosimetry and endoradiotherapy studies. Mol Pharm. 2018;15:5183–91.
111. Timmermand OV, Elgqvist J, Beattie KA, Örbom A, Larsson E, Eriksson SE, et al. Preclinical efficacy of hK2 targeted [177Lu] hu11B6 for prostate cancer theranostics. Theranostics. 2019;9:2129.
112. Gupta A, Shin JH, Lee MS, Park JY, Kim K, Kim JH, et al. Voxel-based dosimetry of iron oxide nanoparticle-conjugated 177Lu-labeled folic acid using SPECT/CT imaging of mice. Mol Pharm. 2019;16:1498–506.
113. Furhang EE, Chui C-S, Sgouros G. A Monte Carlo approach to patient-specific dosimetry. Med Phys. 1996;23:1523–9.
114. Zaidi H. Relevance of accurate Monte Carlo modeling in nuclear medical imaging. Med Phys. 1999;26:574–608.
115. Loudos G, Tsougos I, Boukis S, Karakatsanis N, Georgoulias P, Theodorou K, et al. A radionuclide dosimetry toolkit based on material-specific Monte Carlo dose kernels. Nucl Med Commun. 2009;30:504–12.
116. Dieudonné A, Hobbs RF, Lebtahi R, Maurel F, Baechler S, Wahl RL, et al. Study of the impact of tissue density heterogeneities on 3-dimensional abdominal dosimetry: comparison between dose kernel convolution and direct Monte Carlo methods. J Nucl Med. 2013;54:236–43.
117. Hippeläinen E, Tenhunen M, Sohlberg A. Fast voxel-level dosimetry for 177Lu labelled peptide treatments. Phys Med Biol. 2015;60:6685.
118. Khazaee Moghadam M, Kamali Asl A, Geramifar P, Zaidi H. Evaluating the application of tissue-specific dose kernels instead of water dose kernels in internal dosimetry: a Monte Carlo Study. Cancer Biother Radiopharm. 2016;31:367–79.
119. Lee MS, Kim JH, Paeng JC, Kang KW, Jeong JM, Lee DS, et al. Whole-body voxel-based personalized dosimetry: the multiple voxel S-value approach for heterogeneous media with nonuniform activity distributions. J Nucl Med. 2018;59:1133–9.
120. Lee MS, Hwang D, Kim JH, Lee JS. Deep-dose: a voxel dose estimation method using deep convolutional neural network for personalized internal dosimetry. Sci Rep. 2019;9:10308.
121. Hwang D, Kang SK, Kim KY, Seo S, Paeng JC, Lee DS, et al. Generation of PET attenuation map for whole-body time-of-flight 18F-FDG PET/MRI using a deep neural network trained with simultaneously reconstructed activity and attenuation maps. J Nucl Med. 2019;60:1183–9.
122. Park J, Hwang D, Kim KY, Kang SK, Kim YK, Lee JS. Computed tomography super-resolution using deep convolutional neural network. Phys Med Biol. 2018;63:145011.
123. Hwang D, Kim KY, Kang SK, Seo S, Paeng JC, Lee DS, et al. Improving the accuracy of simultaneously reconstructed activity and attenuation maps using deep learning. J Nucl Med. 2018;59:1624–9.
124. Kang SK, Seo S, Shin SA, Byun MS, Lee DY, Kim YK, et al. Adaptive template generation for amyloid PET using a deep learning approach. Hum Brain Mapp. 2018;39:3769–78.
125. Hegazy MAA, Cho MH, Cho MH, Lee SY. U-net based metal segmentation on projection domain for metal artifact reduction in dental CT. Biomed Eng Lett. 2019;9:375–85.
126. Mansour RF. Deep-learning-based automatic computer-aided diagnosis system for diabetic retinopathy. Biomed Eng Lett. 2018;8:41–57.
127. Cicone F, Gnesin S, Denoël T, Stora T, van der Meulen NP, Müller C, et al. Internal radiation dosimetry of a ^{152}Tb-labeled antibody in tumor-bearing mice. EJNMMI Res. 2019;9:53.
128. Sivapackiam J, Laforest R, Sharma V. ^{68}Ga[Ga]-Galmydar: biodistribution and radiation dosimetry studies in rodents. Nucl Med Biol. 2018;59:29–35.
129. Maina T, Konijnenberg MW, KolencPeitl P, Garnuszek P, Nock BA, Kaloudi A, et al. Preclinical pharmacokinetics, biodistribution, radiation dosimetry and toxicity studies required for regulatory approval of a phase I clinical trial with ^{111}In-CP04 in medullary thyroid carcinoma patients. Eur J Pharm Sci. 2016;91:236–42.
130. Hino-Shishikura A, Suzuki A, Minamimoto R, Shizukuishi K, Oka T, Tateishi U, et al. Biodistribution and radiation dosimetry of [18F]-5-fluorouracil. Appl Radiat Isot. 2013;75:11–7.
131. Repetto-Llamazares AH, Larsen RH, Mollatt C, Lassmann M, Dahle J. Biodistribution and dosimetry of ^{177}Lu-tetulomab, a new radioimmunoconjugate for treatment of non-Hodgkin lymphoma. Curr Radiopharm. 2013;6:20–7.
132. Sakata M, Oda K, Toyohara J, Ishii K, Nariai T, Ishiwata K. Direct comparison of radiation dosimetry of six PET tracers using human whole-body imaging and murine biodistribution studies. Ann Nucl Med. 2013;27:285–96.
133. Stabin MG. Fundamentals of nuclear medicine dosimetry. Springer Science & Business Media; 2008.